

# Resonance Clustering in Globally Coupled Electrochemical Oscillators with External Forcing

István Z. Kiss

*Department of Chemistry, 3501 Laclade Ave.,*

*Saint Louis University, St. Louis, MO 63103*

Yumei Zhai, and John L. Hudson\*

*Department of Chemical Engineering, 102 Engineers' Way,*

*University of Virginia, Charlottesville, VA 22904-4741*

## Abstract

Experiments are carried out with a globally coupled, externally forced population of limit-cycle electrochemical oscillators with an approximately unimodal distribution of heterogeneities. Global coupling induces mutually entrained (at frequency  $\omega_1$ ) states; periodic forcing produces forced-entrained ( $\omega_F$ ) states. As a result of the interaction of mutual and forced entrainment, resonant cluster states occur with equal spacing of frequencies that have discretized frequencies following a resonance rule  $\omega_n \cong n\omega_1 - (n-1)\omega_F$ . Resonance clustering requires an optimal, intermediate global coupling strength; at weak coupling the clusters have smaller sizes and do not strictly follow the resonance rule, while at strong coupling the population behaves similar to a single, giant oscillator.

---

\*Electronic address: hudson@virginia.edu

## I. INTRODUCTION

Rhythms, often generated as synchronization of oscillator populations[1], can also be exposed to external global forcing or feedback. The resulting dynamical behavior depends on the types of oscillators (smooth, relaxation, chaotic), topology of interactions (local, global, or network), and on the magnitude of forcing frequencies relative to the inherent frequencies of the oscillators. A plethora of interesting behavior has been observed with forcing in reaction-diffusion systems or locally coupled, identical oscillators: some examples include labyrinthine standing waves [2], standing wave patterns[3], resonant phase patterns[4], Bloch-front turbulence[5], localized clusters[6], spirals with hypocycloidal trajectories[7], wave traps and twisted spirals[8], and pacemaker entrainments[9].

Less attention has, however, been paid to the analysis of heterogeneous populations of oscillators with a distribution of natural frequencies. A simple example is a globally coupled population with global forcing. Following Kuramoto's heuristic argument[10], it is expected that global coupling would produce a mutually entrained state; this state behaves as a giant oscillator and becomes entrained to the frequency of an external forcing signal. However, the frequency adjustment process of the mutually entrained state is not trivial: Sakaguchi [11] studied the effects of the external fields on mutual entrainment by analysis of a phase model with unimodal heterogeneities. The simulation results show that a transition from the mutual entrainment to the forced entrainment occurs as forcing strength is enhanced; in between, two and more plateaus are seen in the frequency-vs-natural-frequency plots which indicate the formation of multiple, resonance clusters. Because of the interaction of the mutually entrained cluster (with frequency of  $\omega_1$ ) and the forced cluster ( $\omega_F$ ), new resonant clusters with frequency of  $\omega_n \cong n\omega_1 - (n-1)\omega_f$  are formed at weak forcing strengths. Note that these discretized frequencies are equally spaced with  $\Delta\omega = \omega_1 - \omega_f$ . It was also shown that the order parameter exhibits large amplitude oscillations when two major clusters are formed. [11, 12]

In this paper we investigate experimentally resonance clustering in a chemical system (the oscillatory electrodisolution of a nickel electrode array in sulfuric acid solution) with global coupling and forcing with limit cycle oscillators. The mutual and forced entrainment states are identified, and their interactions are analyzed. Features of resonance clustering are compared as coupling strength and forcing amplitude and frequency are varied. Numer-

ical studies are carried out to confirm the experimental finding of resonance clustering in ordinary differential equation models and to investigate the features of the dynamics in a large parameter space.

## II. EXPERIMENTS

### A. Experimental Setup

The experiments were carried out in a standard three electrode electrochemical cell containing 3 mol/dm<sup>3</sup> sulfuric acid at 11 °C with Ni working, a Hg/Hg<sub>2</sub>SO<sub>4</sub>/K<sub>2</sub>SO<sub>4</sub> reference, and a Pt counter electrodes [13, 14]. The currents ( $i_k(t)$ ) of Ni electrodes (64 1-mm diameter electrodes in an 8 × 8 geometry with 2 mm spacing) were measured at 100 Hz. The potential of each electrode was held at potential  $V$  versus Hg/Hg<sub>2</sub>SO<sub>4</sub>/concentrated K<sub>2</sub>SO<sub>4</sub> reference electrode. The external forcing is added to the applied potential  $V(t) = V_0 + b\sin(2\pi f_F t)$ .  $V_0 = 1.09$  V. The electrodes were connected to the potentiostat through one series (collective) resistor,  $R_s$ , and through 64 parallel resistors[13, 14]. The interaction strength  $K$  was controlled through the external resistors  $K = (R_s/R_{\text{tot}})/(1 - R_s/R_{\text{tot}})$  where  $R_{\text{tot}} = 10.1\Omega$  was the total resistance.

The phases and frequencies of the oscillators were determined with the Hilbert transform method [15] from time series data of current  $i_k(t)$  [13]. An order parameter, defined as the normalized vector sum of the phase points ( $P_k(t)$ ) in  $H(i_k(t) - \langle i \rangle)$  vs.  $(i_k(t) - \langle i \rangle)$  space, is used to characterize the extent of the synchrony of the population

$$Z(t) = \frac{\sum P_k(t)}{\sum_k |P_k(t)|}, \quad (1)$$

where  $H$  is the Hilbert transform. This order parameter [13, 16, 17] is similar to the Kuramoto order parameter [10]. The magnitude of  $r = |Z|$ , the order, has a maximum value of 1 for full synchronization and zero for complete desynchronization (for a population of infinite size).

### B. Results

The population in this study has a nearly unimodal natural frequency distribution (without coupling and forcing) with a standard deviation of 8.5 mHz; the frequency histogram

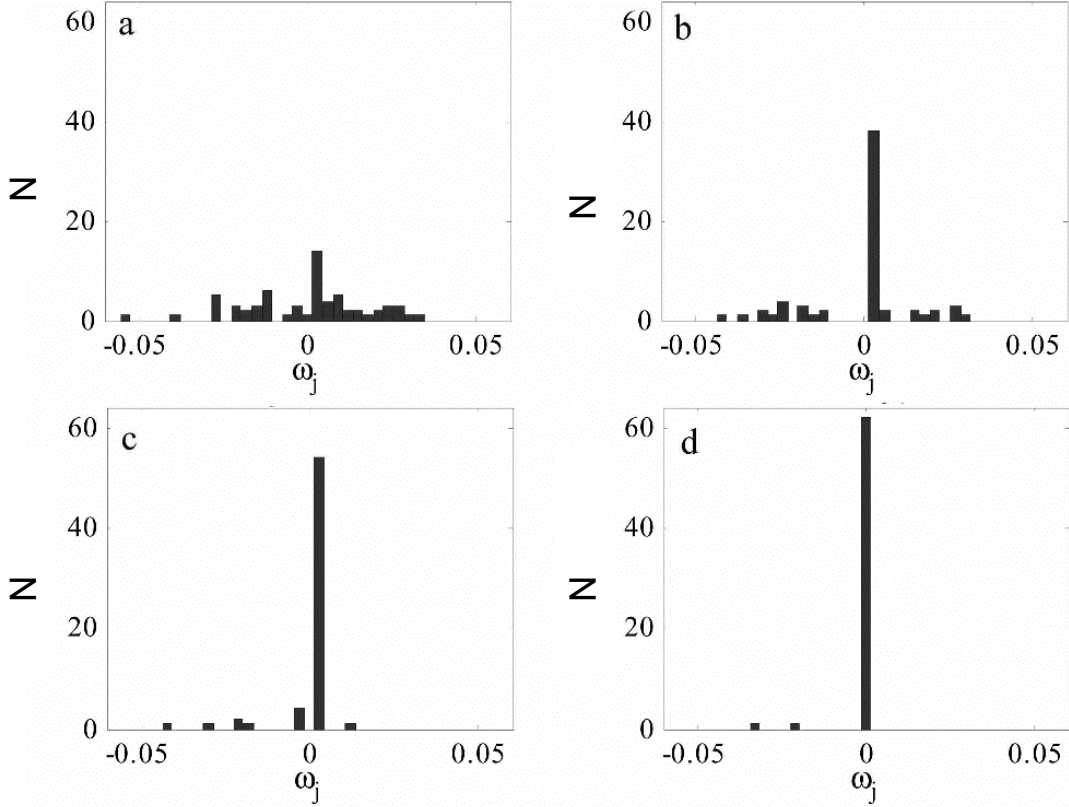


Figure 1: Experiments: Dimensionless frequency histograms ( $\omega = f / \langle f \rangle - 1$ ) at different coupling strengths for a unimodal population. The mean natural frequency  $\langle f \rangle = 0.47\text{Hz}$ , standard deviation  $\sigma = 8.5\text{mHz}$ . (a)  $K = 0$ . (b)  $K = 0.026$ . (c)  $K = 0.031$ . (d)  $K = 0.042$ .

is shown in Fig. 1a. Figs. 1b-d also show the frequency histograms at  $K = 0.026$ ,  $0.031$  and  $0.042$ , respectively. At  $K = 0.026$  (Fig. 1b), a dominant, mutually entrained cluster emerged at approximately the mean natural frequency. Elements with high and low natural frequencies were not entrained yet. With a stronger coupling of  $K = 0.031$  (Fig. 1c), the cluster grew in size considerably and only a few elements were left out. At  $K = 0.042$  (Fig. 1d), 62 out of the 64 elements had been in the same cluster with two elements of lower natural frequencies desynchronized. External periodic forcing was applied to all these three partially synchronized states.

First consider the forcing of the most synchronized state at  $K = 0.042$ . Without forcing a mutually entrained cluster of 62 elements formed at  $\omega_1 = 0.450\text{ Hz}$ . The periodic forcing was applied at a higher frequency of  $\omega_F = f_F = 0.47\text{Hz}$ . With forcing amplitude of  $b = 3.3\text{mV}$  some elements of the original (mutually entrained) cluster moved out and formed a new

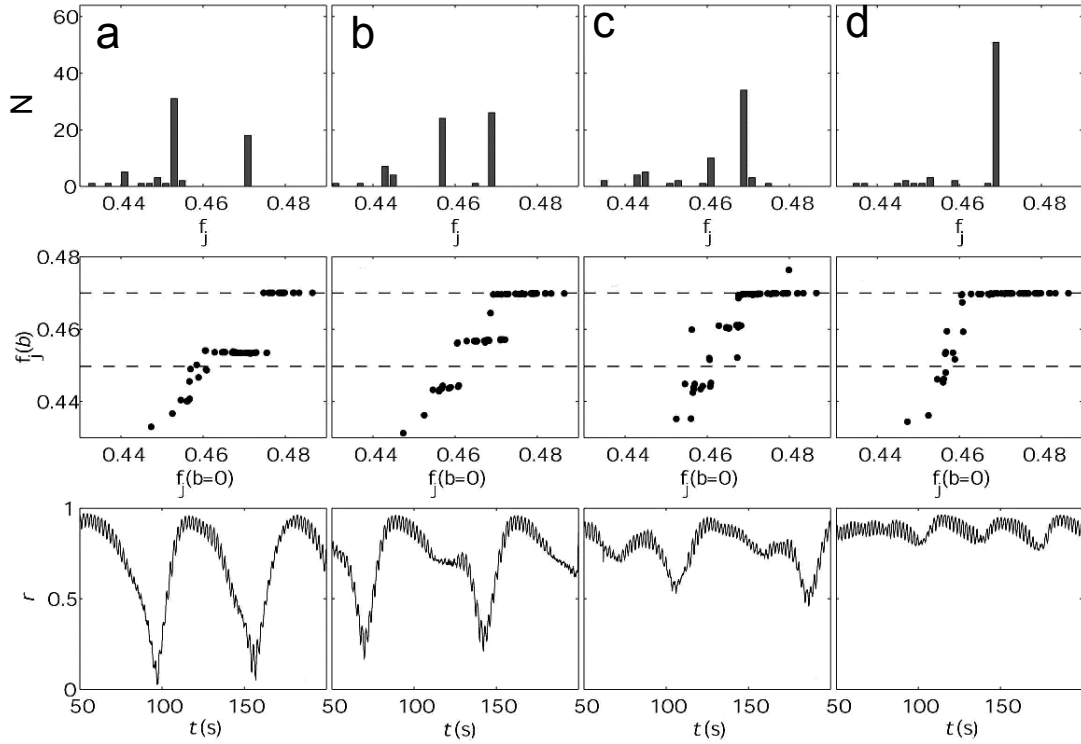


Figure 2: Experiments: Periodic forcing on a unimodal population with  $K = 0.042$ .  $V_0 = 1.09\text{V}$ . Mean frequency before forcing  $\langle f \rangle = 0.4497$  Hz, forcing frequency  $f_F = 0.47\text{Hz}$ ,  $f_F - \langle f \rangle > 2\sigma$ . Top row: Frequency histograms at different forcing amplitudes. Middle row: Frequencies in presence of coupling and forcing versus the corresponding natural frequencies. Upper and lower dashed line are  $f_F$  and  $\langle f \rangle$ , respectively. Bottom row: Time series of order  $r$ . a.  $b = 3.3\text{mV}$ . b.  $b = 4.0\text{mV}$ . c.  $b = 4.6\text{mV}$ . d.  $b = 5.3\text{mV}$ .

cluster at the forcing frequency (forced entrainment). In Fig. 2a (frequency histogram, top panel) there were two large peaks corresponding to the two clusters. The plot of frequencies-vs-natural-frequencies (middle panel) also clearly shows two plateaus; the one of the forced entrainment was at  $f_F$  while the other one of the mutual entrainment had a frequency that is slightly higher than the mean frequency without forcing. The order oscillated in large amplitudes at  $b = 3.3\text{mV}$  (bottom panel). As  $b$  increased to  $4.0\text{mV}$ , the forced entrained cluster grew in size; simultaneously two mutual entrained clusters emerged (Fig. 2b). The frequency of the old mutual entrained cluster ( $\omega_1$ ) further increased to be closer to  $\omega_F$ . A new, small resonant cluster formed at  $\omega_2 = 2\omega_1 - \omega_F$ . With a even stronger forcing of  $b = 4.6\text{mV}$ , more resonant clusters formed at frequencies of  $\omega_n \cong n\omega_1 - (n-1)\omega_F$ ,  $n = 2, 3, 4$  (Fig. 2c).

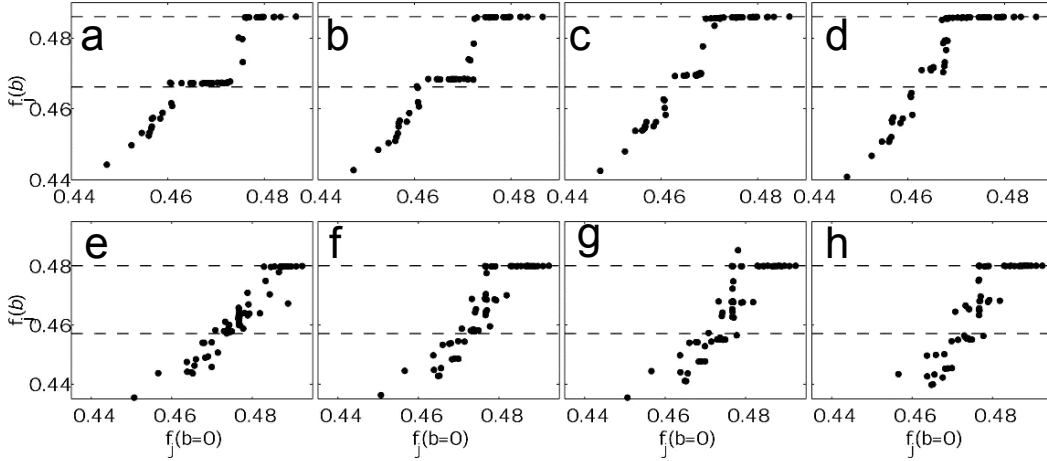


Figure 3: Periodic forcing on a unimodal population with weak coupling strengths. Frequencies in presence of coupling and forcing versus the corresponding natural frequencies. Top row:  $K = 0.031$ ,  $\langle f \rangle = 0.466\text{Hz}$ ,  $f_F = 0.486\text{Hz}$ . a.  $b = 3.3\text{mV}$ . b.  $b = 4.0\text{mV}$ . c.  $b = 4.6\text{mV}$ . d.  $b = 5.3\text{mV}$ . Bottom row:  $K = 0.026$ ,  $\langle f \rangle = 0.4571\text{Hz}$ ,  $f_F = 0.48\text{Hz}$ . e.  $b = 3.3\text{mV}$ . f.  $b = 4.95\text{mV}$ . g.  $b = 5.3\text{mV}$ . h.  $b = 5.95\text{mV}$ . Upper and lower dashed line are  $f_F$  and  $\langle f \rangle$ , respectively.

However, each of these clusters had a smaller size compared with the two mutual entrained clusters at  $b = 4.0\text{mV}$  (Fig. 2b). With only one large cluster the order no longer exhibited large amplitude oscillations. Note that the spacing between any adjacent clusters became smaller as  $b$  increased. When the forcing amplitude was further increased to  $b = 5.3\text{mV}$ , no distinct resonant clusters were observed and only one large, the forced entrained cluster, appeared with 12 non-entrained elements scattering in the lower frequency region (Fig. 2d). Finally, with strong enough forcing amplitude, all the elements formed one cluster at the forcing frequency (not shown).

During the periodic forcing of a less synchronized state obtained at  $K = 0.031$  (Fig. 1c), the occurrence of resonant clusters requires stronger forcing strengths as shown in Figs. 3a-d. Forced entrainment occurred with forcing and two main clusters coexisted at weak forcing strengths (Figs. 3a, b). As  $b$  increases, the forced entrained cluster grew larger (Figs. 3a-d) and finally became the only dominant cluster at  $b > 5.3\text{mV}$ . The third, new resonant cluster with the frequency of  $\omega_2 = 2\omega_1 - \omega_F$  appeared at  $b = 4.0\text{mV}$ ; however, compared with the case of  $K = 0.042$  at the same weak forcing strength (Fig. 2f), the new cluster was much smaller and can be barely seen (Fig. 3b). The presence of the third cluster only became

obvious at a greater forcing amplitude of  $b = 4.6\text{mV}$  (Fig. 3c); in contrast, in the case of  $K = 0.042$  at  $b = 4.6\text{mV}$  multiple resonant clusters had emerged (Fig. 2c). Because of the small size of the resonant cluster, the existence of two main clusters at  $b = 4.6\text{mV}$  the order oscillated in large amplitudes (not shown). At  $b = 5.3\text{mV}$ , the forcing was strong enough to induce multiple resonant clusters with closer equal frequency spacing (Fig. 3d) and with smaller sizes. Again, before the system reached a fully forced entrainment state (not shown in the figures) the mutual entrainment clusters completely disappeared by giving some of their elements to the forced entrainment cluster while leaving the others nonentrained.

The forcing experiments were carried out for an even less synchronized population of oscillators obtained with  $K = 0.026$  (Fig. 1b). With a small forcing strength of  $b = 3.3\text{ mV}$  (Fig. 3e), a high peak arose at the forcing frequency in the frequency histogram ; however, the mutual entrained cluster had broken up because of the weak coupling. In the frequency-vs-natural-frequency plot below the forced entrained plateau, the frequencies of the nonentrained elements formed an almost continuous  $45^\circ$  line in the lower frequency region with a small shoulder around  $0.4571\text{ Hz}$  (which is close to the mean natural frequency of the oscillators). The order exhibited fairly large oscillations but these oscillations were not regular (not shown). As  $b$  was increased to a quite strong value of  $4.95\text{mV}$ , the elements with lower frequencies started to form multiple small groups as shown in Fig. 3f. However, these 'clusters' were small and close to each other on the  $45^\circ$  line in the frequency-vs-natural-frequency plot (Fig. 3f). Small clusters were also observed at stronger forcing strengths  $b = 5.3\text{mV}$  (Fig. 3g ) and  $b = 5.95\text{mV}$  (Fig. 3h). Since there was no second large cluster besides the forced entrained one, the order oscillations were irregular with relatively small amplitudes (not shown). Finally, a completely forced entrained cluster was formed with strong enough forcing amplitudes.

### III. NUMERICAL SIMULATIONS

#### A. Model Equations

We used a model of anodic electrodisolution of a single nickel electrode proposed by Haim et al. [18]. The model in a dimensionless form involves two variables: the dimensionless double layer potential drop ( $e$ ) and the surface coverage of  $\text{NiO}+\text{NiOH}$  ( $\theta$ ). One oscillator

is described by the following two equations:

$$\frac{de}{dt} = \frac{V - e}{R} - i_F(\theta, e) \quad (2)$$

$$\Gamma \frac{d\theta}{dt} = \frac{\exp(0.5e)}{1 + C_h \exp(e)} (1 - \theta) - \frac{BC_h \exp(2e)}{cC_h + \exp(e)} \theta \quad (3)$$

where  $V$  is the dimensionless applied potential,  $R$  is the dimensionless series resistance,  $\Gamma$  is the surface capacity, and  $i_F$  is the Faradaic current:

$$i_F(\theta, e) = \left( \frac{C_h \exp(0.5e)}{1 + C_h \exp(e)} + a \exp(e) \right) (1 - \theta) \quad (4)$$

The parameter values  $C_h = 1600$ ,  $a = 0.3$ ,  $B = 6 \times 10^{-5}$ ,  $c = 1 \times 10^{-3}$  were optimized [18] to obtain dynamical features similar to experiments.

In the experiments the oscillators are inherently different because of electrode heterogeneities [19] and because of addition of different individual external resistors. We model the non-identical nature of the oscillators by giving the oscillators different values for the parameters  $R$  and  $\Gamma$  in Eqs. 2 and 3. (Other choices are also possible, however, these parameters best approximate the experiments.[16, 17]) For element  $k$  the resistance and the surface capacitance are obtained using the relationships  $R_k = (1 + \Delta_k)R_0$  and  $\Gamma_k = (1 + \Delta_k)\Gamma_0$ , where  $\Delta_k$  is a heterogeneity parameter and  $R_0$  and  $\Gamma_0$  are the mean values. We used a fixed value of  $\Gamma_0 = 0.01$ , and  $R_0 = 20$  throughout this study. We choose a Lorentzian distribution for  $\Delta_k$ . (For comparison, simulations with global coupling were also made with a Gaussian distribution.[17]) The Lorentzian distribution  $p(x) = \gamma / \{\pi[(x - x_0)^2 + \gamma^2]\}$  is characterized by a parameter  $\gamma$ ;  $2\gamma$  is the half-width of the distribution. For a typical value of  $\gamma = 0.5$ , the equation parameters  $R_k$  and  $\Gamma_k$  vary within a range of 5% of their means.

Electrical global coupling of strength  $K$  is considered; the model for the coupled set of  $N$  oscillators is then[16, 17]:

$$\frac{de_k}{dt} = \frac{V - e_k}{R_k} - i_{F,k}(\theta_k, e_k) + \frac{1}{R_0} K (e_{mean}(t) - e_k) \quad (5)$$

$$\Gamma_k \frac{d\theta_k}{dt} = \frac{\exp(0.5e_k)}{1 + C_h \exp(e_k)} (1 - \theta_k) - \frac{BC_h \exp(2e_k)}{cC_h + \exp(e_k)} \theta_k \quad (6)$$

where  $R_0$  is the mean resistance. Global coupling occurs because of the presence of mean potential ( $e_{mean}(t) = 1/N \sum_{k=1}^N e_k(t)$ ) in Eq. 5.  $K = 0$  represents uncoupled oscillators;  $K \rightarrow \infty$  yields maximum global coupling that synchronizes the oscillators. Global forcing

is added through the circuit potential:

$$V(t) = V_0 + b \sin(2\pi f_F t), \quad (7)$$

where  $V_0 = 15$  is a set potential,  $b$  and  $f_F = 0.0745$  are the forcing amplitude and frequency, respectively. A variable step size fourth order Runge-Kutta method of Matlab was used to integrate Eqs. 5 and 6 with a display step size of  $\Delta t = 0.5$ , absolute error =  $10^{-6}$ , relative error =  $10^{-3}$ . Smaller step sizes and error limits gave the same results. A transient of  $t = 10000$  was discarded from each time series.

The phases and frequencies of simulated oscillators are determined from time series data of  $e_k(t)$  with the Hilbert transform method[15].

## B. Results

Without global coupling and forcing the oscillators exhibit frequencies determined by the introduced heterogeneities, as shown in Fig. 4a. Since the heterogeneities are small, the frequencies of the oscillators follow almost linearly the heterogeneities and thus the frequency distribution is similar to a Lorentzian distribution. With global coupling only, a mutually entrained state occurs (see Fig. 4b) above a critical coupling strength  $K_c$ [10, 13, 16, 17, 20]; in this mutually entrained state a large fraction of the oscillators are synchronized. When the coupling strength is increased above  $K_c$ , the number of mutually entrained oscillators increases until all the 64 oscillators are fully synchronized. With global forcing only, (see Fig. 4c), as the forcing amplitude increases more and more oscillators lock to the forced entrainment state. Note however, that there is no phase transition, and the increase in the number of entrained oscillators with forcing amplitude is determined by the frequency distribution; the large increase at around  $b = 0.6$  is due to the large number of oscillators of similar frequencies (peak in Fig. 4a).

With both global coupling and forcing, in a large fraction of the parameter space  $(K, b)$ , each oscillator can be classified as belonging to one of the three major groups: desynchronized (D), mutually entrained (M), and forced entrained (F) states. Fig. 4d shows the regions in the  $(K, b)$  parameter space in which these states can occur. At low forcing and coupling the system is desynchronized (D). Starting from this desynchronized state with increasing coupling there is a transition to the occurrence of the mutually entrained state (M+D in

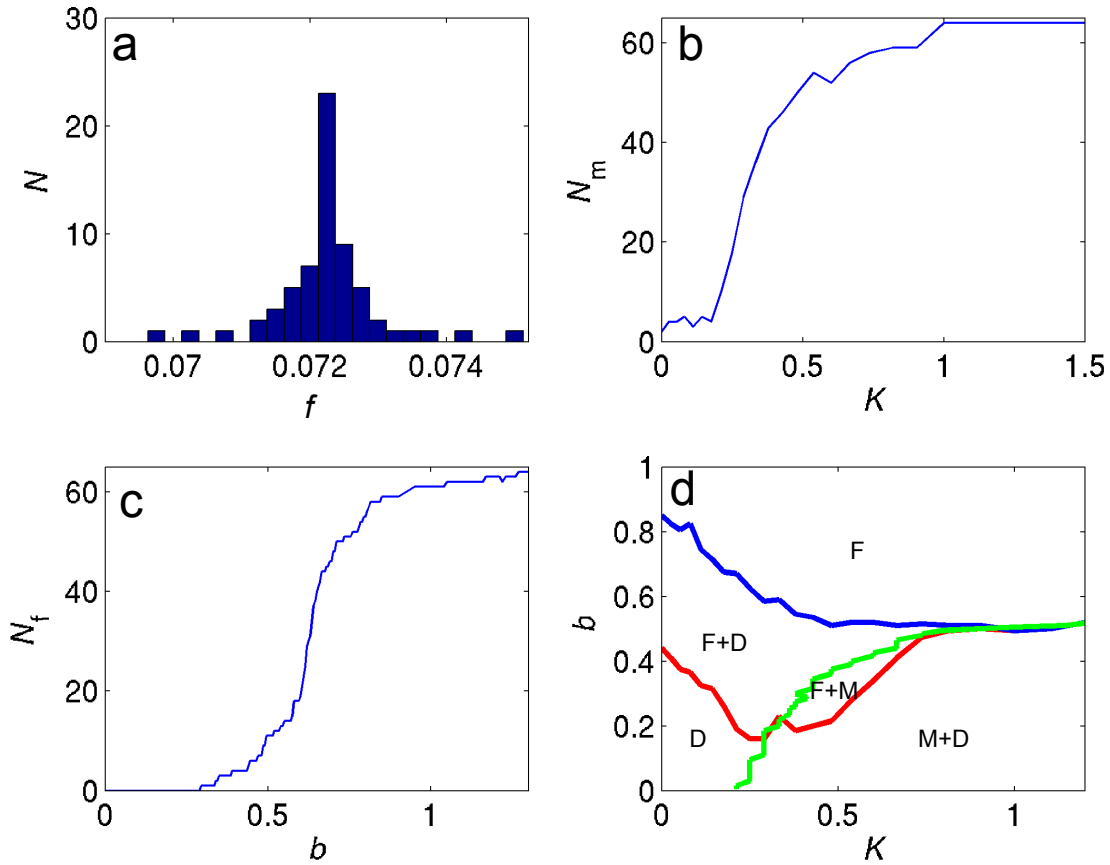


Figure 4: (Color Online) Numerical Simulations: Mutual and forced entrainment in a model of sixty-four globally coupled oscillators with external forcing. a. Natural (inherent) frequency distribution. b. Mutual entrainment with global coupling only. Number of mutually entrained oscillators vs. coupling strength  $K$ . c. Forced entrainment with external forcing only. Number of oscillators locked to external forcing signal vs. forcing amplitude  $b$ . d. Phase diagram showing forced and mutually entrained regions in the coupling strength – forcing amplitude parameter space. F: Forced entrainment. M: Mutual entrainment. D: desynchronized state.  $f_F = 0.0745$ .

Fig. 4b). With increasing the forcing amplitude in a weakly coupled population, a forced entrainment state starts to occur (F+D). At very strong coupling, the transition is similar to the forcing of a single oscillator: the frequency of the mutually entrained cluster (M) shifts to that of the forcing (F).

We investigated the dynamics in the middle region of the phase diagram further, where both forced and mutually entrained states can co-exist. (Note that this is not hysteresis. In a synchronized state some of the oscillators are mutually, some are forced entrained; there

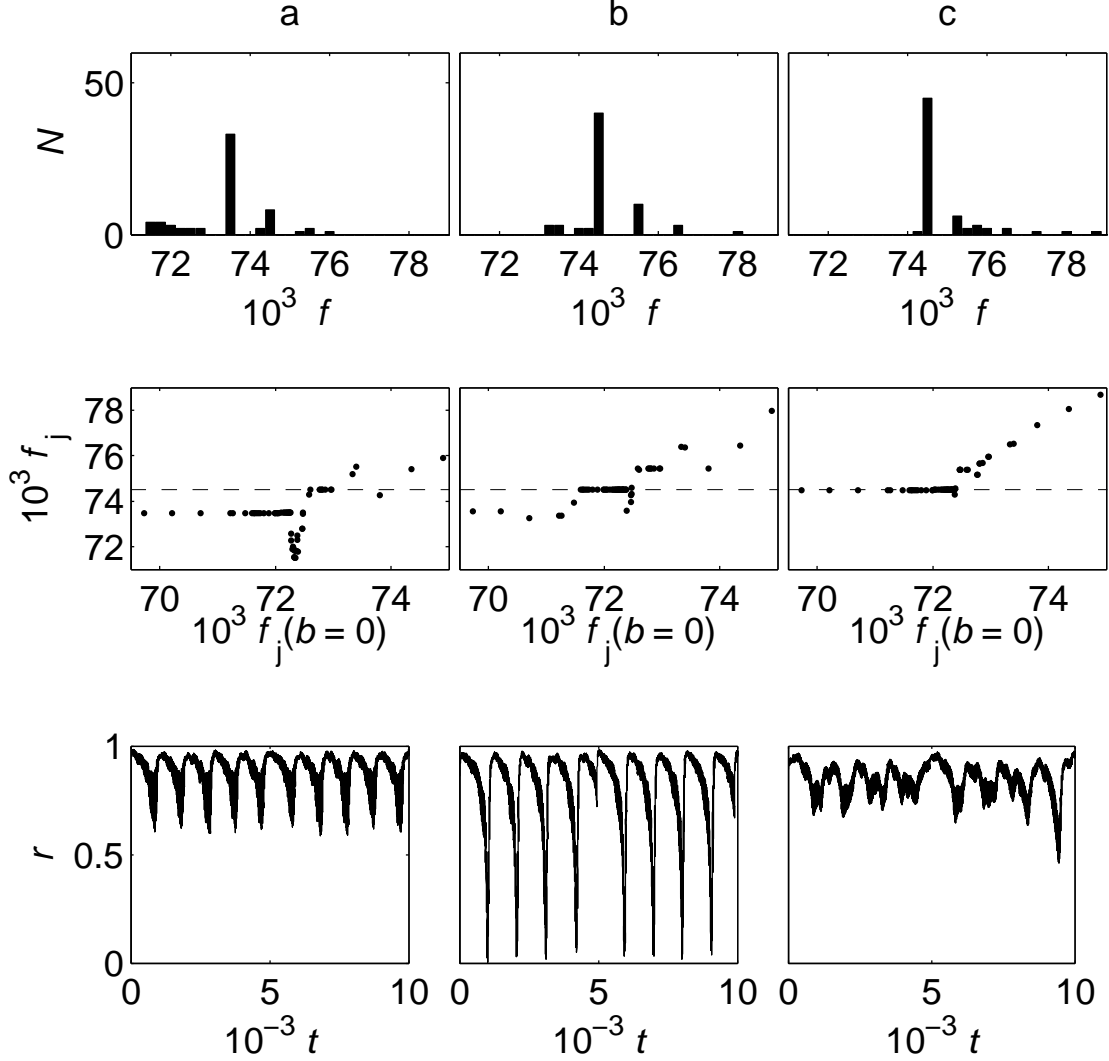


Figure 5: Numerical Simulations: frequency distributions and order parameters at  $K = 0.67$ . Top row: frequency distribution of oscillators. Middle row: frequency of oscillators vs. inherent frequency (dashed line denotes the forcedly entrained cluster). Bottom row: order parameter vs. time. a. Mutual entrainment dominated state with weak forcing.  $b = 0.428$ . b. Resonance clustering at intermediate forcing strength.  $b = 0.443$ . c. Entrainment to strong forcing.  $b = 0.452$ .

are some oscillators that are also entrained but, as we shall see below, their frequencies are combination of those of the mutually and forced entrainment states.) The frequencies and the order of such a state with weak forcing is shown in Fig. 5a. Since the forcing is weak, the large peak in the frequency histogram is associated with the mutually entrained state, while the smaller peak at the forcing frequency with the forced entrainment. The frequency

vs. inherent frequency graph (middle) shows that the elements with lower frequencies form the mutually entrained state; such an asymmetry in the entrainment was also observed with pure coupling as well. [16] Elements with frequencies between the mutually and forced entrainment groups have strongly scattered, lower frequencies; those oscillators with larger frequencies are not entrained. Because the majority of the population is mutually entrained, a large value of order parameter (bottom panel) is observed with small modulation due to forced entrainment state.

At a somewhat stronger forcing amplitude, a restructuring of the frequencies of the oscillators occurs (see Fig. 5b). Now the major group is associated with the forced entrainment, however, the mutually entrained state is difficult to determine since the population becomes clustered at frequencies with a (dimensionless) spacing of approximately 0.0009 [ $f = \{0.0736, 0.0745$  (forcing),  $0.0754, 0.0764\}$ ]; 8 elements of the population of 64 oscillators do not belong to these resonant clusters. Resonant clusters seem to appear as an interaction between the mutual and forced entrainments and produce a strongly oscillating order parameter.

As the forcing amplitude is further increased, the forced entrainment (Fig. 5b) state dominates in which the elements around the forcing frequencies along with those of the lower frequencies are entrained and the elements with higher frequencies are not synchronized. The order parameter again has a large, close to 1 value, but with small fluctuations due to the desynchronized elements.

Resonance clustering to a lesser extent also appears at weaker coupling strength as it is shown at three forcing amplitudes in Fig. 6. At these conditions (Figs. 6ab), the elements do form various frequency clusters, however, there may be quite a few clusters with smaller number of elements and the spacing between the clusters is small. These states also exhibit oscillating order (not shown in the figures). At a state very close the destruction of mutual entrainment (Fig. 6c) the frequencies of mutual and forced entrainment states are very close and frequency clustering appears as discretized frequencies of groups of 1-3 oscillators only.

Fig. 7 shows the simulation results with a population of 512 oscillators at inherent frequency distribution, coupling strength, and forcing amplitude similar to those investigated with 64 oscillators. We observed five frequency clusters with approximate spacing of 0.001 [at frequencies  $f = \{0.0734, 0.0745$  (forcing),  $0.0756, 0.0766, 0.0777\}$ ]. This 5-cluster state with  $N = 512$  is reminiscent of the 4-cluster state with  $N = 64$  (Fig. 5b), however, one

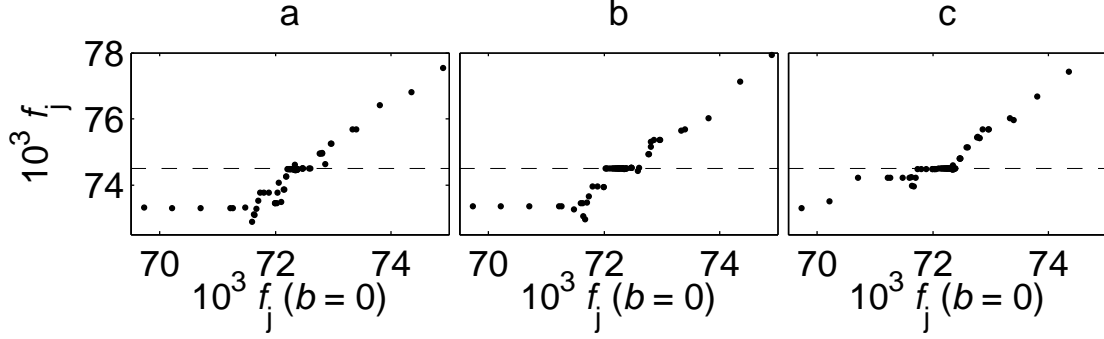


Figure 6: Numerical simulations: frequencies of oscillators (with coupling and forcing) vs. inherent frequencies at weaker interactions,  $K = 0.54$ . a. Weak forcing.  $b = 0.385$ . b. Intermediate forcing strength.  $b = 0.398$ . c. Strong forcing.  $b = 0.410$ .

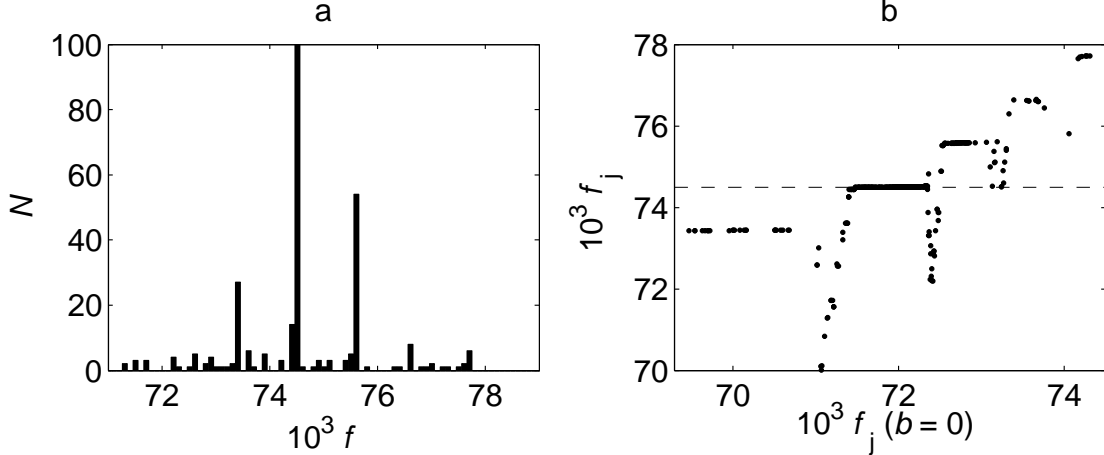


Figure 7: Numerical simulations: population of 512 oscillators exhibiting resonance clustering at  $K = 0.67$  and  $b = 0.47$ . a. Frequency distribution of oscillators. (For  $f = 0.075$  there is a large peak with  $N = 325$ , therefore, a zoom is shown) b. Frequency of oscillators vs. inherent frequency (dashed line denotes the forcing frequency).

additional cluster could be resolved at  $f = 0.0777$ . Thus, the fine structure of resonance clusters can be better seen with larger populations.

#### IV. DISCUSSION

Clustering is a behavior of a population of oscillators through which dynamically differentiated elements form. The classification of clusters [21] is based on whether it affects mainly

the phases (phase clusters)[22, 23] or the amplitudes (amplitude clusters)[24] of the periodic oscillators. Chaotic systems are particularly inclined for producing clusters at coupling strengths weaker than those required for identical synchronization[25, 26, 27]. In this study, we observed frequency clusters in a forced, weakly coupled population of limit-cycle electrochemical oscillators with unimodal heterogeneities. In addition to the trivial mutually and entrained clusters, groups of elements are obtained at other, discrete frequency values. We also showed that at coupling strengths and forcing amplitudes with well-defined resonance clusters the frequencies are equally spaced and follow the relationship found by Sakaguchi [11]:  $\omega_n \cong n\omega_1 - (n - 1)\omega_F$ . (Such spectrum was analyzed by linear stability of the forced entrainment state.[28]) With weaker coupling strengths a large number of clusters with small number of elements were observed whose frequency was not greatly modified from the natural frequencies. We note that frequency discretization through a different mechanism, *viz.*, through large delays in the coupling term, was also observed in a pair of lasers [29]and in a pair chaotic Rössler oscillators[30].

Along with the occurrence of frequency clusters, a strongly oscillating order parameter was observed; the order decreased to very low values and thus intermittent loss of the overall rhythm could be observed. The loss of the overall rhythm may have implications in the dynamics of biological systems where the rhythm could be either essential or pathological [1].

A biological example in which coupling and forcing play a role is the circadian master clock in the brain[31]; the suprachiasmatic nuclei consist of heterogeneous, circadian oscillators that are entrained by cell interactions and by external light. The SCN is strongly heterogeneous and the interaction of the core, being entrained by light, and the shell (composed of mostly self-oscillating neurons) is a complex issue[32, 33]; resonance clustering could play a role in the dynamical behavior of the different regions. Resonant interactions between oscillators have been considered as well in the context of information processing with oscillatory units [34, 35]; the cortex is considered as a weakly coupled oscillator population forced by the thalamic input.

As far as the importance of resonance clustering in biological networks of rhythmic elements is concerned, we shall consider that we investigated a global coupling topology. Although such global, all-to-all coupling is not very likely in biological systems, sometimes a network of oscillators can be approximated by global coupling. A fundamental communi-

cation mechanism of bacteria, quorum sensing, is often modeled by global interactions; such a mechanism was shown to be able to produce synchrony[36]. Synchronization of circadian cells was modeled by a global interaction mechanism based on an argument that the spatial transmission of neurotransmitters released by each cell is fast compared to the timescale of oscillations[37]. Neural networks with electrically spiking neurons are also often can be considered as a population of weakly, coupled globally coupled oscillators[38]. Even when network coupling occurs, the depth of the network is often not very large when external forcing is effective[39] thus global coupling approximation and resonance clustering can play a role in generation of collective dynamics with coupling and forcing.

Some features of the cluster interactions such as generation of the resonant clusters could also be observed in a population with bimodal heterogeneities; the forced system can be regarded as a simplified case of bimodal system where one special mode has standard deviation of zero and its strength can be directly controlled. Frequency clustering and generation of complex collective signal were found with the global coupling of periodic electrochemical oscillator populations with bimodal natural frequency distributions[40]; merging and splitting of clusters occurred on the way to the final synchronized state with increasing the coupling strength. Such bimodal (and multimodal) populations may occur in biological systems that are composed of broadly heterogeneous cell groups.

Although we investigated resonance clustering here with electrochemical oscillators, similar dynamical differentiation mechanisms are expected to occur in a variety of rhythmic multicellular systems under the co-operative effects of coupling and forcing; the synchronized groups of elements would contribute to the formation of multi-structured hierarchical organizations often seen in complex systems[41, 42].

## Acknowledgments

Financial support from the National Science Foundation (CBET-0730597) is acknowledged.

- 
- [1] A. T. Winfree, *The geometry of biological time* (Springer-Verlag, New York, 1980).
  - [2] V. Petrov, Q. Ouyang, and H. L. Swinney, *Nature* **388**, 655 (1997).

- [3] A. von Oertzen, H. H. Rotermund, A. S. Mikhailov, and G. Ertl, *J. Phys. Chem. B* **104**, 3155 (2000).
- [4] A. L. Lin, M. Bertram, K. Martinez, H. L. Swinney, A. Ardelea, and G. F. Carey, *Phys. Rev. Lett.* **84**, 4240 (2000).
- [5] B. Marts, A. Hagberg, E. Meron, and A. L. Lin, *Phys. Rev. Lett.* **93**, 108305 (2004).
- [6] V. K. Vanag, A. M. Zhabotinsky, and I. R. Epstein, *Phys. Rev. Lett.* **86**, 552 (2001).
- [7] O. Steinbock, V. Zykov, and S. C. Müller, *Nature* **366**, 322 (1993).
- [8] O. Rudzick and A. S. Mikhailov, *Phys. Rev. Lett.* **96**, 018302 (2006).
- [9] H. Fukuda, N. Tamari, H. Morimura, and S. Kai, *J. Phys. Chem. A* **109**, 11250 (2005).
- [10] Y. Kuramoto, *Chemical oscillations, waves and turbulence* (Springer, Berlin, 1984).
- [11] H. Sakaguchi, *Prog. Theoret. Phys.* **79**, 39 (1988).
- [12] E. Montbrio, J. Kurths, and B. Blasius, *Phys. Rev. E* **70**, 056125 (2004).
- [13] I. Z. Kiss, Y. M. Zhai, and J. L. Hudson, *Science* **296**, 1676 (2002).
- [14] I. Z. Kiss, W. Wang, and J. L. Hudson, *J. Phys. Chem. B* **103**, 11433 (1999).
- [15] A. S. Pikovsky, M. G. Rosenblum, and J. Kurths, *Synchronization: A Universal Concept in Nonlinear Science* (University Press, Cambridge, 2001).
- [16] Y. M. Zhai, I. Z. Kiss, and J. L. Hudson, *Ind. Eng. Chem. Res.* **43**, 315 (2004).
- [17] Y. M. Zhai, I. Z. Kiss, H. Daido, and J. L. Hudson, *Physica D* **199**, 387 (2004).
- [18] D. Haim, O. Lev, L. M. Pismen, and M. Sheintuch, *J. Phys. Chem.* **96**, 2676 (1992).
- [19] I. Z. Kiss, W. Wang, and J. L. Hudson, *J. Phys. Chem. B* **103**, 11433 (1999).
- [20] A. T. Winfree, *J. Theor. Biol.* **16**, 15 (1967).
- [21] A. S. Mikhailov and K. Showalter, *Phys. Rep.* **425**, 79 (2006).
- [22] D. Golomb, D. Hansel, B. Shraiman, and H. Sompolinsky, *Phys. Rev. A* **45**, 3516 (1992).
- [23] K. Okuda, *Physica D* **63**, 424 (1993).
- [24] V. Hakim and W. J. Rappel, *Phys. Rev. A* **46**, R7347 (1992).
- [25] K. Kaneko, *Phys. Rev. Lett.* **63**, 219 (1989).
- [26] K. Kaneko and I. Tsuda, *Complex Systems: Chaos and Beyond* (Springer, Berlin, 2001).
- [27] W. Wang, I. Z. Kiss, and J. L. Hudson, *Chaos* **10**, 248 (2000).
- [28] T. M. Antonsen Jr, R. T. Faghieh, M. Girvan, E. Ott, and J. Plutig, submitted to *Chaos* (arXiv:0711.4135) (2008).
- [29] H. J. Wünsche, S. Bauer, J. Kreissl, O. Ushakov, N. Korneyev, F. Henneberger, E. Wille,

- H. Erzgräber, M. Peil, W. Elsässer, et al., Phys. Rev. Lett. **94**, 163901 (2005).
- [30] S. Yanchuk, Phys. Rev. E **72**, 036205 (2005).
- [31] S. M. Reppert and D. R. Weaver, Nature **418**, 935 (2002).
- [32] M. C. Antle and R. Silver, Trends in Neurosciences **28**, 145 (2005).
- [33] W. Nakamura, S. Yamazaki, N. N. Takasu, K. Mishima, and G. D. Block, J. Neurosci. **25**, 5481 (2005).
- [34] F. C. Hoppensteadt and E. M. Izhikevich, Biosystems **48**, 85 (1998).
- [35] F. C. Hoppensteadt and E. M. Izhikevich, Phys. Rev. Lett. **82**, 2983 (1999).
- [36] J. Garcia-Ojalvo, M. B. Elowitz, and S. H. Strogatz, Proc. Natl. Acad. Sci. USA **101**, 10955 (2004).
- [37] D. Gonze, S. Bernard, C. Waltermann, A. Kramer, and H. Herzl, Biophys. J. **89**, 120 (2005).
- [38] H. Kori, Phys. Rev. E **68**, 021919 (2003).
- [39] H. Kori and A. S. Mikhailov, Phys. Rev. Lett. **93**, 254101 (2004).
- [40] A. S. Mikhailov, D. H. Zanette, Y. M. Zhai, I. Z. Kiss, and J. L. Hudson, Proc. Nat. Acad. Sci. USA **101**, 10890 (2004).
- [41] S. C. Manrubia, A. S. Mikhailov, and D. H. Zanette, *Emergence of Dynamical Order: Synchronization Phenomena in Complex Systems* (World Scientific, Singapore, 2004).
- [42] K. Kaneko, *Life: An Introduction to Complex System Biology* (Springer, 2006).